DOI:10.1111/j.1365-2125.2007.02974.x

Population pharmacokinetic analysis of carboxyhaemoglobin concentrations in adult cigarette smokers

Carol Cronenberger, Diane R. Mould, Hans-Juergen Roethig[1] & Mohamadi Sarkar[1]

Projections Research Inc., Phoenixville, PA and [1]Philip Morris USA Research Center, Richmond, VA, USA

What is already known about this subject

- The pharmacokinetics of carboxyhaemoglobin have been reported previously, primarily with regard to poisoning and toxicity.
- Most of these reports have involved noncompartmental analysis of data obtained where the actual dose of carbon monoxide was not known.

What this study adds

- This study presents a comprehensive population pharmacokinetic model for carboxyhaemoglobin in adult cigarette smokers.
- Since carboxyhaemoglobin is a marker of cigarette smoke exposure, model-based evaluations can be used for simulation and other evaluations of the kinetics of this agent.

Correspondence
Mohamadi Sarkar, MPharm, PhD,
Director of Clinical Pharmacology and Adjunct Associate Professor, MCV/VCU Department of Pharmaceutics, Philip Morris USA, 615 Maury Street, Richmond, VA 23224, USA.
Tel: + 1 804 274 3262
Fax: + 1 804 274 2891
E-mail:
mohamadi.sarkar@pmusa.com

Keywords
carboxyhaemoglobin, FTC, population pharmacokinetics

Received
10 November 2006
Accepted
19 April 2007

Aims
To develop a population-based model to describe and predict the pharmacokinetics of carboxyhaemoglobin (COHb) in adult smokers.

Methods
Data from smokers of different conventional cigarettes (CC) in three open-label, randomized studies were analysed using NONMEM (version V, Level 1.1). COHb concentrations were determined at baseline for two cigarettes [Federal Trade Commission (FTC) tar 11 mg; CC1, or FTC tar 6 mg; CC2]. On day 1, subjects were randomized to continue smoking their original cigarettes, switch to a different cigarette (FTC tar 1 mg; CC3), or stop smoking. COHb concentrations were measured at baseline and on days 3 and 8 after randomization. Each cigarette was treated as a unit dose assuming a linear relationship between the number of cigarettes smoked and measured COHb percent saturation. Model building used standard methods. Model performance was evaluated using nonparametric bootstrapping and predictive checks.

Results
The data were described by a two-compartment model with zero-order input and first-order elimination with endogenous COHb. Model parameters included elimination rate constant (k_{10}), central volume of distribution (Vc/F), rate constants between central and peripheral compartments (k_{12} and k_{21}), baseline COHb concentrations (c0), and relative fraction of carbon monoxide absorbed (F1). The median (range) COHb half-lives were 1.6 h (0.680–2.76) and 30.9 h (7.13–367) (α and β phases, respectively). F1 increased with increasing cigarette tar content and age, whereas k_{12} increased with ideal body weight.

Conclusion
A robust model was developed to predict COHb concentrations in adult smokers and to determine optimum COHb sampling times in future studies.

Introduction

There are more than 4000 chemicals found in cigarette smoke [1]. Cigarette smoking is associated with an increased incidence of both respiratory and cardiovascular disease [2], but the relationship of specific constituents with disease has not yet been established. Carbon monoxide (CO) is one of the cigarette smoke constituents that has a very high affinity for haemoglobin (Hb) relative to that for oxygen (approximately 200-fold [3, 4]). This results in an acute effect of decrease in oxygen-carrying capacity of Hb and a leftward shift of the oxyhaemoglobin dissociation curve [5], which reduces the release of oxygen to tissues. CO also binds with other haemoproteins such as myoglobin, which abounds in skeletal muscles, causing dysfunction by impairing its oxygen-carrying capacity and the transportation of oxygen from the blood to the mitochondria [3, 6].

CO exposure is often estimated by either CO concentrations in exhaled breath or from CO bound to Hb. There are several reports in the literature [7–10] regarding mathematical modelling of carboxyhaemoglobin (COHb) in humans, but none in adult smokers. Some of the models, e.g. the Coburn–Forster–Kane (CFK) equation [11], were developed to predict the rate of endogenous CO production, which has also been used to predict the rate of COHb formation during inhalation exposure to CO [7, 12]. Cigarette smoking involves multiple short and rapid inhalations over the entire smoking period, resulting in a COHb steady state, followed by a period when there is no smoking, resulting in dissociation of CO from haemoglobin. This process has not been systematically characterized in the population of smokers. Since it is not practical to obtain extensive blood sampling from a large population of adult smokers, a population pharmacokinetic (PK) analysis approach was employed. The objectives of this population PK analysis were to characterize the PK and variability of COHb concentrations in adult smokers, and to identify factors which influence COHb disposition.

Methods

Study conduct

This analysis examined data from adult smokers of different conventional cigarettes in three open-label, randomized, controlled, forced-switching, parallel group studies. These studies were conducted to evaluate the effect of switching adult smokers to test cigarettes; however, only the data from smokers of conventional reference cigarettes and those who stopped smoking were used for the model building. The studies were conducted at MDS Pharma Services Inc., Lincoln, Nebraska after approval of the study protocol by the local Internal Review Board. After signing the informed consent and passing screening for inclusion/exclusion criteria, adult male and female smokers of 10–30 conventional cigarettes [Federal Trade Commission (FTC) tar delivery 11 mg (CC1) or 6 mg (CC2)] per day were enrolled. Subjects were confined to the clinic during the entire course of the studies.

Materials

The products used in these studies were: CC1, *Marlboro Lights* cigarettes, tar = 11 mg, nicotine = 0.8 mg, CO = 12 mg; CC2, *Marlboro Ultra Lights* cigarettes, tar = 6 mg, nicotine = 0.5 mg and CO = 7 mg; CC3, *Merit Ultima* cigarettes, tar = 1 mg, nicotine = 0.1 mg and CO = 4 mg. The tar values reported were based on FTC smoking methods.

Study design

Study 1 examined healthy adults who smoked CC1 at baseline ($n = 100$). Following baseline investigations, subjects were randomly assigned to continue to smoke CC1 ($n = 20$), switch to CC3 ($n = 20$) or to stop smoking ($n = 20$) over a period of eight consecutive days. Study 2 included data from 50 healthy adults who smoked CC2 at baseline and were subsequently randomized to continue smoking their original brand ($n = 25$) or to stop smoking ($n = 25$) for a period of 8 days. In study 3, data were used from healthy adult smokers of CC1, of whom 40 were randomized either to continue smoking CC1 ($n = 20$) or to stop smoking ($n = 20$) for 8 days.

Days −2 and −1 were designated as an acclimatization phase, which was followed by randomization to respective smoking groups on day 1. The study design did not include a day 0. During the acclimatization phase subjects were monitored for cigarette consumption in order to determine their daily allotment of cigarettes for the remainder of the study. Subjects continued with their assigned smoking groups through the end of day 8. COHb percentage saturations were evaluated at 07.00, 11.00, 15.00, 19.00 and 23.00 h on baseline (day −1) and day 8 in study 1 and on days −1, 3 and 8 in studies 2 and 3. Smoking was controlled (as described by Roethig *et al*. [13]) and monitored in all three studies. All three studies collected several biomarkers, but only COHb concentrations were evaluated in this modelling analysis.

Analytical methods

COHb quantification Blood samples (10 ml) for determination of COHb concentrations were drawn in K_3EDTA vacutainer tubes at protocol-specified times. COHb in whole blood was assayed spectrophotometrically with a CO oximeter (IL Multi-4; Instrumentation

Laboratory, Lexington, MA, USA) at Covance Central Clinical Laboratory (Indianapolis, IN, USA). Anticoagulated whole blood was aspirated into the CO-oximeter, mixed with diluent, haemolysed with a non-ionic surfactant and brought to a constant temperature in the cuvette. Absorbance of a monochromatic light source passed through the cuvette was measured at six specific wavelengths. The limit of quantification was 0.3%, linear calibration range was 0.3–64.7%. The between-run precision (% coefficient of variation) was <5%.

Machine yield of carbon monoxide The amount of CO formed and tar content of each cigarette type were determined under the experimental conditions under FTC conditions, reported in detail elsewhere [14], carried out at Philip Morris Product Testing Laboratories (Richmond, VA, USA). Briefly, cigarettes were smoked in a Filtrona/Cerulean Smoking Machine (Cerulean Corp., Richmond, VA, USA), models 400-450, equipped with harmonized smoking hood and CO analyser. The standard test protocol was used utilizing 35 ml puff volume over a 2-s puff duration collected every 60 s. CO was analysed in the mainstream smoke by Fourier transform infrared spectroscopy connected to the smoke machine.

Data analysis

Creating the database The final database used for this analysis consisted of 1960 COHb percent saturation observations obtained from 190 subjects. Smoking history, machine yield tar and CO concentrations (FTC conditions), time and duration for each cigarette smoked, demographics and COHb data from all three studies were combined into a single database. Smoking information consisted of the FTC tar and CO yield per cigarette, as well as time and duration of each cigarette smoked in two studies, and the total number of cigarettes smoked per day for the third study. Therefore, for approximately two-thirds of the subjects, each cigarette smoked was treated as a separate dose record. For the remaining individuals (study 3), all cigarette consumption was assumed to occur over a 12-h period.

Since all subjects were confirmed smokers and required to smoke the reference cigarette for at least 4 weeks prior to enrolment as part of the inclusion criteria, they were assumed to be at steady state with regard to COHb concentrations prior to study entry. Each cigarette was assumed to provide a unit dose of COHb, which implies an assumption of a linear relationship between the cigarette and parts per million (p.p.m.) CO available for inhalation, as well as a linear relationship between p.p.m. CO and COHb percent saturation [15]. Law *et al*. have reported [15] that the relationship between the biochemical markers of smoking and the number of cigarettes smoked is approximately linear for consumption of up to 20 cigarettes per day. For heavy smokers (>20 cigarettes/day) the relationship was no longer linear and exposure was lower than anticipated. For the purpose of this evaluation, in which subjects were enrolled who smoked ≤30 cigarettes a day, the assumption of linearity is supported.

The effect of possible covariates included in the model were age, body weight, ideal body weight (IBW [16]), body mass index (BMI), gender and race. FTC tar was examined only as a covariate on the relative fraction of CO absorbed. Other covariates, such as age and body weight, were examined for potential effect on the rate constants and baseline COHb, in addition to the relative fraction of CO absorbed (F1). The addition of a covariate was accepted only if it resulted in a reduction in the objective function by at least 10.8 points ($P < 0.001$). In addition, the criteria for the addition of a covariate factor included improvement in one or more of the following: prediction of the observed COHb percent saturation, minimization of the interindividual variance terms, and reduction in the magnitude of the residual variability.

Pharmacokinetic analysis COHb percent saturation–time data were analysed using the nonlinear mixed-effects modelling program, NONMEM, v.5, Level 1 [17, 18] with the Compaq Digital Visual Fortran 6.6C compiler. The First Order Conditional Estimation (FOCE) method with interaction was implemented for all models tested because the comparison of objective functions (likelihood ratio test) from nested models is not reliably χ^2 distributed under the first order (FO) method [19, 20], whereas the FOCE method with interaction is generally more reliable for such comparisons. Standard model-building approaches were employed during model development [21]. Several structural models, including one- and two-compartment models with different input functions, were investigated during this evaluation. A structural model was identified, followed by refinement of the variance–covariance matrix, and then covariate identification.

Final model evaluation

Once a final model was identified, a nonparametric bootstrap analysis was performed to establish 95% confidence intervals (CI) for parameter estimates [22]. Additionally, a limited visual predictive check [23] was conducted for representative individuals in each FTC group using the final model. Individuals were selected in order to represent key covariates adequately, such as age,

IBW and the number of cigarettes smoked per day. Dense sample times were generated for the individuals in these visual predictive check databases. Two hundred and fifty simulated replicates were generated, and the 95% prediction intervals were calculated from the Winsorized distributions [24, 25] of the simulated data. Winsorizing is a method used to eliminate possible outliers by setting the values equal to, or more extreme than a selected quantile to that of the selected quantile. By trimming the data in this fashion, the distorting effects of influential outliers could be abrogated prior to further processing. Winsorizing also preserves the general distributional characteristics of the data. Following the generation of these intervals, the observed data were overlaid on the prediction intervals and the distributions of observed and simulated data were visually compared.

Results

A listing of the baseline demographic information for the subjects in this study is provided in Table 1. The final model for COHb was a two-compartment model with zero-order input and first-order elimination. The parameters of the base model included the elimination rate constant (k_{10}), the rate constant describing transfer of COHb from the central to the peripheral compartment (k_{12}), the rate constant describing COHb transfer from the peripheral to the central compartment (k_{21}), the central volume of distribution uncorrected for the relative fraction of CO absorbed (Vc/F) and relative fraction of CO absorbed (F1). A baseline (endogenous) concentration (c0) was also estimated as a parameter for the base structural pharmacokinetic model. Interindividual variability was described using an exponential error model for k_{12}, k_{21} and F1, and covariance between these same parameters. The residual variability was described using a combined additive and constant coefficient of variation (CCV) model. The population means of the final model parameter estimates and 95% CIs are displayed in Table 2. The parameters for the final COHb model are defined below (Equations 1–6).

$$k_{10} = \theta_1$$

$$k_{12} = \left(\theta_3 \bullet \left(\frac{IBW}{70} \right)^{\theta_2} \right) \bullet \exp^{(\eta_{k12})}$$

$$k_{21} = \theta_4 \bullet \exp^{(\eta_{k21})}$$

$$\mathrm{C0} = \theta_6$$

$$\mathrm{F1} = \left(\frac{FTC}{10} \right)^{\theta_5} \bullet \left(\frac{AGE}{55} \right)^{\theta_7} \bullet \exp^{(\eta_{F1})}$$

$$\frac{Vc}{\mathrm{F}} = \theta_8$$

Table 1
Summary of baseline demographic information for the carboxyhaemoglobin database ($N = 190$)

Baseline characteristics	Mean (SD)	Median (range)
NumCig*	20 (4.6)	20 (8–29)
Age (years)	33 (11)	30 (21–63)
Height (cm)	173 (8.4)	173 (152–190)
Weight (kg)	73 (11)	72 (48–108)
IBW (kg)	73 (11)	72 (49–108)
BMI (kg m^{-2})	24 (3.0)	24 (18–33)
Gender	93 male, 97 female	
Race	185 White, 5 non-White	

**NUMCIG is the reported number of cigarettes smoked per day. IBW, Ideal body weight; BMI, body mass index.*

In addition to FTC tar, the amount of CO formed under these smoking conditions (FTC CO) was examined as a predictor of COHb 'dose' via the relative fraction of CO absorbed (F1). There was little difference between FTC tar and FTC CO as covariates, i.e. $\theta_5 = 0.277$ (FTC CO) *vs*. 0.163 (FTC tar). Additionally, the interindividual variability for F1 was the same (26.0% CV), therefore FTC tar was retained in the model. For the reference 70-kg, 55-year-old, White male subject, k_{12} was predicted to be 0.211 h^{-1}. Predictions for the elimination rate constant (k_{10}) and k_{21} were estimated to be 0.151 h^{-1} and 0.0665 h^{-1}, respectively. Endogenous COHb saturation was predicted to be 0.423%, while the prediction for Vc/F was 1.13 l. The median (range) half-lives calculated from individual parameter estimates were approximately 1.6 h (0.680–2.76) and 30.9 h (7.13–367) for the distributive and terminal phases, respectively.

As observed in Figure 1, there was a visual trend towards increasing values of interindividual variability (e.g. individual η value) associated with F1 with increases in FTC tar in the base model (left panel). Age showed a positive trend with F1 in the base model as well. There was also a positive relationship (Figure 1) between IBW and the rate constant describing distribution of COHb into the peripheral compartment (k_{12}) in the base model. These visual trends in the η plots were generally resolved in the final model (Figure 1, right panels) for all covariates with little or no apparent change in the individual η values despite changing covariate values. This suggests that these covariate influences were accounted for in the final model. Plots of observed, typical (population) and individual predicted COHb

Table 2
Final model parameter estimates and 95% confidence intervals for carboxyhaemoglobin model

Parameter (units)	Population mean (95% CI*)	Interindividual variability (CV%)
k_{10} (h^{-1})	0.151 (0.143, 0.164)	NE
k_{12} (h^{-1})	0.211 (0.189, 0.261)	41.5 (30.7, 56.8)
Effect of IBW	1.29 (0.881, 1.86)	
k_{21} (h^{-1})	0.0665 (0.0421, 0.148)	129 (56.1,163)
c0 (percent saturation)	0.423 (0.399, 0.444)	NE
F (%)	1 FIX	26.0 (21.6, 30.3)
Effect of FTC	0.163 (0.0799, 0.246)	
Effect of age	0.213 (0.0301, 0.335)	
Vc/F (l)	1.13 (1.13, 1.24)	NE
Random residual error as CV%	12.2 (10.9, 13.5)	
Random residual additive error (%)	0.158 (0.135, 0.192)	

**95% CI obtained from nonparametric bootstrap evaluation. NE, Not evaluated.* $k_{10} = \theta_1$; $k_{12} = \theta_3 \times (\text{ideal body weight}/70)^{\theta_2}$; $k_{21} = \theta_4$; $c0 = \theta_6$; $F = 1 \times (FTC/10)^{\theta_5} \times (Age/55)^{\theta_7}$; $Vc/F = \theta_8$. *FTC, Federal Trade Commission.*

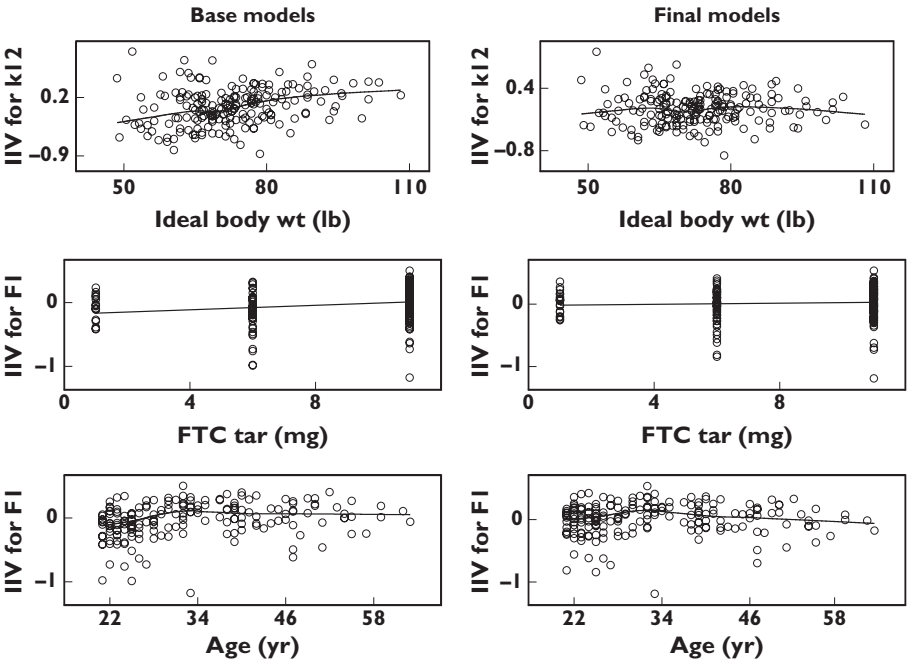

Figure 1
Relationship between ideal body weight and interindividual variability (IIV or η) for k_{12}, Federal Trade Commission (FTC) tar content and IIV for relative fraction of carbon monoxide absorbed (F1), and age and IIV for F1 from the final carboxyhaemoglobin model. The circles are observed data and the solid line is a loess smooth added to facilitate visualization of the trend in the data

percent saturation *vs*. time for the base and final model for an individual from the FTC6 group are provided in Figure 2, and are representative of subjects in all FTC groups. As can be seen in Figure 2, the agreement between the typical predicted COHb concentrations and the observed data is improved in the final model (lower panel) compared with the base model (upper panel). The mean (SD) model-predicted COHb percent saturations over the course of an average day for the different smoking groups included in this analysis are displayed in Figure 3. There is good agreement between the model predicted and observed mean data. Diagnostic plots for the final model are displayed in Figure 4. Figure 4A displays a plot of observed vs. typical (population)

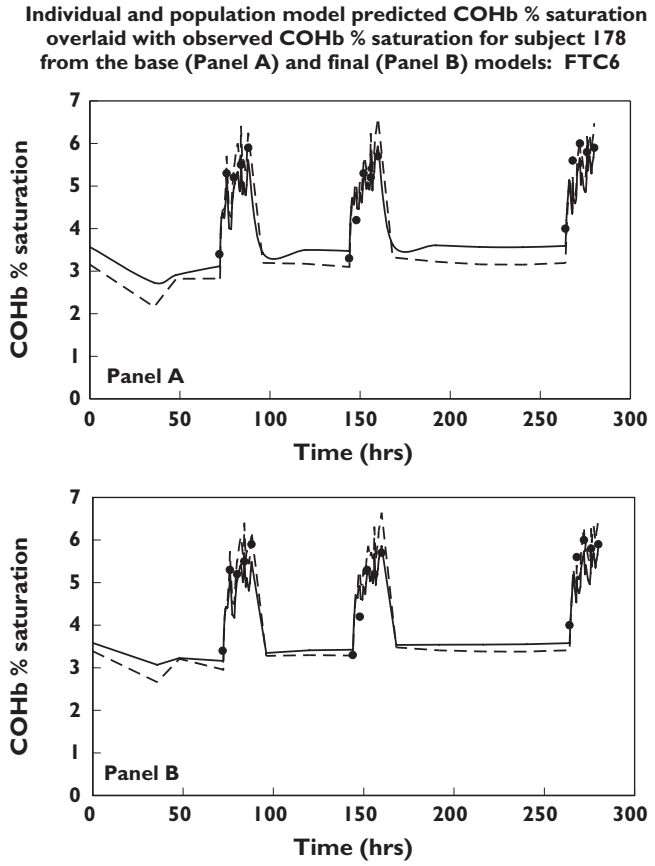

Figure 2

Diagnostic plots for a representative individual from the Federal Trade Commission 6 group. The filled circles are observed data, the dashed line is the population (typical) predicted curve and the solid line is the individual predicted curve. (Individual Predicted, (——) Population Predicted, (– –) Observed, (●))

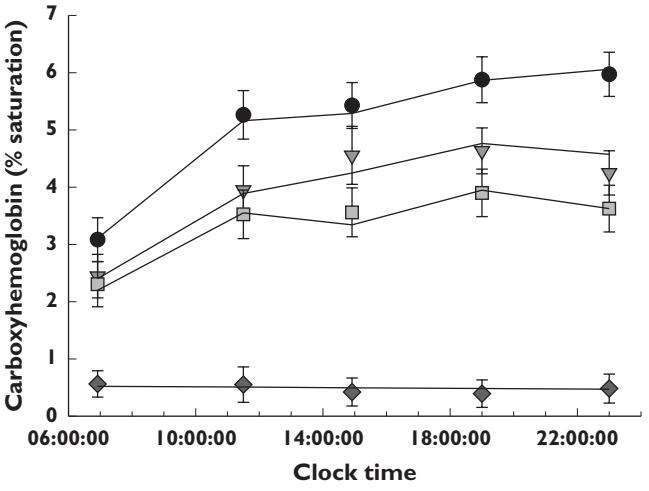

Figure 3

Mean typical predicted and observed carboxyhaemoglobin (COHb) percentage saturation based on the final COHb model. The symbols represent the observed mean (SD) COHb percentage saturation and the solid line depicts the population (typical) predicted COHb percentage saturation from the final model. (CC1, (●); CC2, (▽); CC3, (■); Non-smoking, (◆) Individual Predicted, (——))

predicted COHb percent saturation. In general, the data are uniformly scattered about the line of unity, although there does appear to be a slight underprediction at the higher COHb percent saturations. Figure 4B displays the weighted residuals *vs*. typical predicted COHb percent saturation; the data are uniformly scattered about zero, with the majority of observations falling between –4 and +4. Results of the predictive check for all of the FTC groups are illustrated in Figure 5. The majority of observed COHb concentrations fell within the 95% prediction intervals for all of the FTC groups, with an approximately equal distribution of observed data across the interval. The mean values obtained for the simulated data are generally consistent with the central values for the observed data. Overall, the model performance appeared to be acceptable for this model.

Discussion

This study has described a population-based pharmacokinetic model that was developed to predict COHb concentrations in adult smokers. The final model (Equations 1–7) was a two-compartment model based on a zero-order input function (constant input rate) and first-order distribution and elimination. The model converged successfully and generated estimates of standard errors for all parameters that were <30%. In addition, nonparametric bootstrap analysis demonstrated that the 95% CIs were generally narrow and centered about the parameter estimates.

Important physiological and chemical processes involved in the distribution and elimination of CO were taken into consideration during development of this model. The primary function of Hb is to serve as an oxygen transport protein within the systemic circulation. Haemoglobin is a tetrameric structure consisting of two α and two β chains which surround a protoporphyrin IX and Fe^{2+} complex (haeme). In addition to binding with dissolved oxygen in the blood, Hb also binds in a slowly reversible fashion with CO to form COHb. CO binds to Hb with an affinity estimated to be in the range of 200–250 times greater than that reported for oxygen [5, 26].

The disposition of exogenous CO occurs in a manner similar to that observed for oxygen [27]. On inhalation, CO diffuses rapidly across the alveolar membrane and

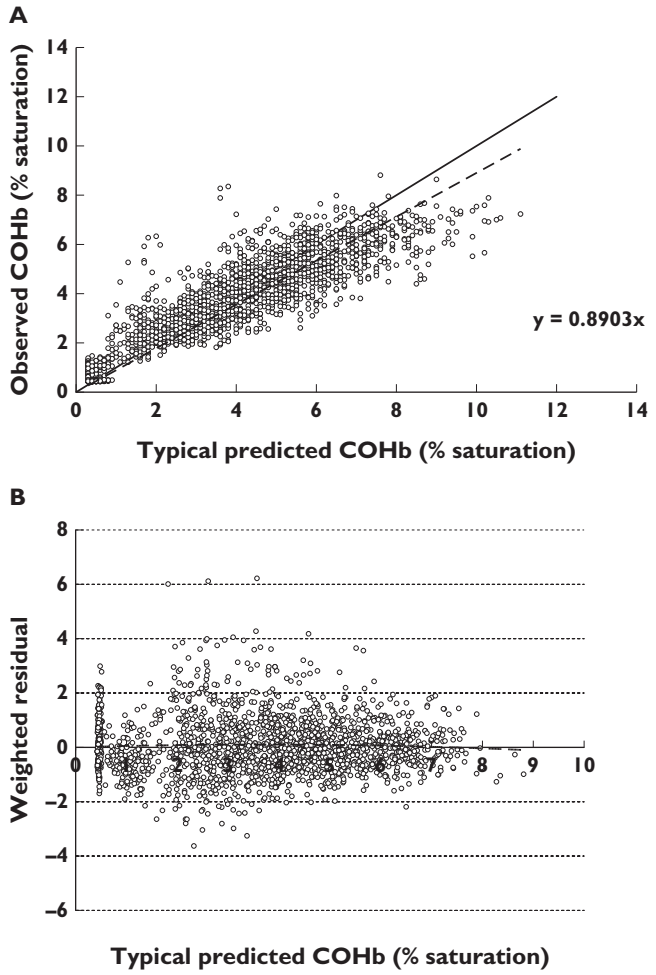

Figure 4

Diagnostic plots for the final carboxyhaemoglobin (COHb) pharmacokinetic model. (A) Population (typical) predicted *vs*. observed COHb percentage saturation. (Data, (○); (B) Weighted residuals *vs*. observed COHb percentage saturation. Line of Unity, (——); Linear Regression, (– –))

binds with Hb in the pulmonary capillary blood. CO is then distributed by Hb (as COHb) throughout the systemic circulation, where it diffuses across the venous capillaries into peripheral tissues and binds with other haemeproteins, e.g. myoglobin [28, 29] in muscle, cytochrome P-450 [30] and cytochrome *c* oxidase [31, 32]. Myoglobin is a monomeric haeme protein found mainly in muscle tissue, where it serves as an intracellular storage site for oxygen. CO binds coordinately to haeme iron atoms in a manner similar to that of oxygen [29]. The binding of CO to haeme in the myoglobin, although not as strong as that for Hb, is still much stronger than that of oxygen (~20–50 times) and much higher than for the other haemeproteins. Once the exogenous source is removed, CO is eliminated from the body via expired air in the lungs following its dissociation from Hb in the pulmonary capillaries.

There are several mathematical models in the literature that have attempted to describe the absorption, distribution and elimination of CO [12,33]. The CFK mono-exponential equation [11] is probably the most widely used equation which takes into account CO concentration in inhaled air, duration of exposure and alveolar ventilation. However, this model was developed to determine the rate of endogenous CO production, which has been used to predict the rate of COHb formation during inhalation exposure to CO. Furthermore, the model was developed based on exposure to a fixed concentration of CO. Since smoking-related exposure to CO is a highly variable process, primarily depending on the smoking behaviour and type of cigarette smoked, most of the models reported in the literature do not apply to the case of CO exposure from cigarette smoking.

The current model was developed by taking into consideration the variable input function by accounting for each cigarette as an individual input (whenever the data were available). Based on the model predictions developed, the typical COHb concentrations in smokers were reasonably predicted between 07.00 and 23.00 h, as shown in Figure 3. COHb concentrations reach a steady state after about 10–12 h. In general, the predicted and observed COHb concentrations are in good agreement and appear to be consistent throughout the day.

Smokers in the current study experienced COHb concentrations that ranged from 0.8 to 11.1% saturation, which is consistent with the 1–15% saturation range reported in the literature [10, 15, 34, 35]. In the current analysis, baseline COHb saturation in adult smokers who were randomized to the nonsmoking group was predicted to be approximately 0.42%, which is consistent with literature estimates of <1.5% and 1–3% saturation for nonsmokers [10, 15, 34, 35].

For years the disposition of COHb has typically been reported to be monoexponential, as described by the CFK equation [11]. However, both Wagner [36] and Shimazu [33] have proposed that the elimination of CO is consistent with biexponential decay, as observed in dogs and a CO-poisoned patient, respectively. In addition, Bruce and Bruce [9] fitted a multicompartmental model to experimental data obtained from healthy male subjects for whom multiple COHb concentrations were available, and for whom CO exposure conditions were carefully controlled. The subjects were exposed only to room air between and following CO administration. CO elimination from the blood was biphasic and the terminal elimination half-life was dependent upon CO

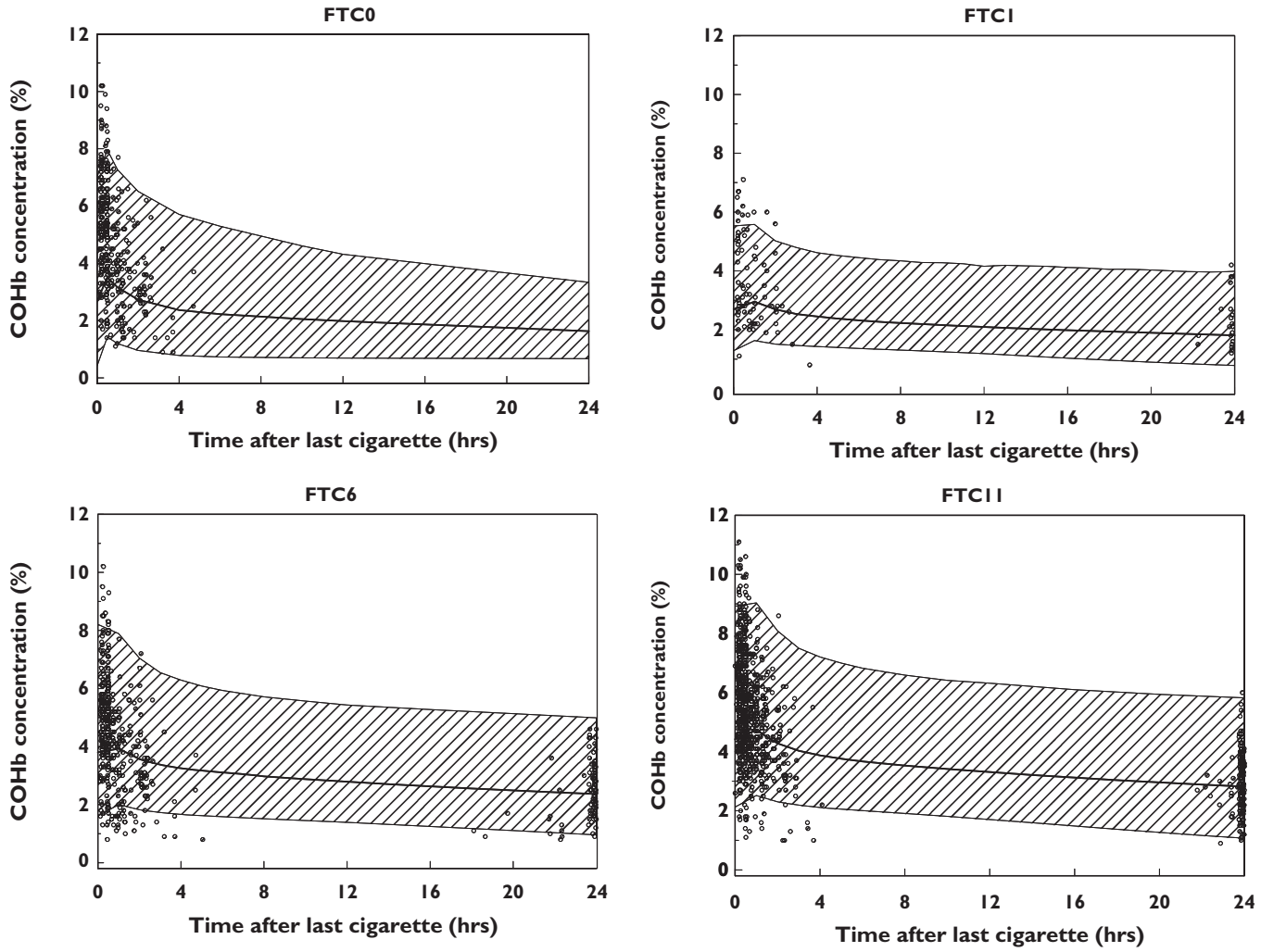

Figure 5

Visual predictive checks. Observed carboxyhaemoglobin (COHb) concentrations overlaid on the 95% prediction intervals for Federal Trade Commission (FTC) 0 (nonsmoking) group, the FTC1 group, the FTC6 group and the FTC11 group. The area containing the hashed lines represents the 95% prediction intervals, the solid line the median of the prediction interval, and the triangles the observed COHb percentage saturation data

exposure duration, CO concentration, peak COHb concentrations and subject-specific parameters. Employing three different methods for calculation of mean COHb half-lives, Bruce and Bruce observed a range of 208–358 min (3.47–5.97 h). Unfortunately, the sampling duration for COHb following cessation of CO administration was only 259 min (4.32 h), therefore the estimates for half-life must be interpreted with caution, particularly as there is a significant distribution phase incorporated in this estimation process. If COHb were to continue to decline at the same rate over an extended sampling duration, the half-life estimate would be accurate. However, if the COHb rate of elimination were to occur more slowly, the half-life could be underpredicted.

The median terminal half-life for COHb in the current analysis was estimated to be approximately 31 h, which is considerably longer than previously reported literature values. However, the disposition of COHb has not been fully characterized in adult smokers. Almost all of the published half-life values for COHb were derived from patients who experienced CO poisoning [9, 33, 37]. In these cases where CO poisoning occurred, the half-life of COHb ranged from approximately 74 to 137 min (e.g. 1.23–2.28 h). One possible explanation for the discrepancy in the elimination time lies in the treatment for CO poisoning, which typically employs supplemental oxygen[13] [38], or treatment within a hyperbaric oxygen chamber [37, 39, 40]. Due to the increase in the partial

pressure of oxygen (pO_2) as a result of these treatments, the dissociation of CO from Hb is facilitated [38]. The enhanced elimination which results is evidenced by a shorter half-life for COHb [41] and suggests that there is a clinical benefit obtained from the use of a hyperbaric chamber to treat cases of CO poisoning. In addition, many of the half-life determinations reported in the literature for COHb need to be interpreted with caution because of sparse data collection and inadequate sampling duration [7, 40, 41]. As the subjects in the current analysis stopped smoking, the longer terminal elimination half-life observed for COHb in this case is more likely to be a reflection of the 'true' dissociation of CO from Hb and subsequent elimination from the body under natural conditions; i.e. exposure to ambient air.

It might be speculated that smokers may have physiological characteristics which affect their ability to eliminate CO, such as differences in dynamic lung function and airway resistance [42]. In addition, it is known that smokers have higher concentrations of Hb compared with subjects who have never smoked [43], which could ultimately influence the capacity for elimination of CO. Furthermore, additional sources of variability, such as the proportion of the cigarette smoked and the depth of inhalation, have not been investigated in this analysis and would be expected to contribute to the intersubject variability, which was still rather high for some parameters.

The COHb model from the current analysis predicts an increase in k_{12} with IBW. One possible explanation for this effect is that heavier subjects typically have larger blood volumes [44]. A larger blood volume would imply a greater quantity of Hb, therefore heavier subjects would theoretically carry a higher CO load at any given COHb percent saturation. A higher CO load would lead to a greater partial pressure of CO in blood being delivered to the periphery, thus enabling it to dissociate from Hb at a faster rate upon reaching the lower partial pressures at the peripheral tissues [44, 45]. Subjects with higher body weights also have greater cardiac outputs [46], thus enabling them to deliver CO to the tissues at a faster rate.

The interindividual variability for the fraction of CO absorbed was high, which may be due in part to individual smoking habits. The fraction of the cigarette smoked, the depth of inhalation and other factors could reasonably influence the extent of CO absorption. The COHb model also predicted an apparent effect of FTC tar and FTC CO on the fraction of CO absorbed. Both cigarettes with higher tar content and cigarettes that produced more CO as a function of FTC tar rating were associated with an increased COHb F1. Additionally, the current model predicts that the fraction of CO absorbed has a modest positive relationship to age. Although a positive correlation between age and COHb has been reported in the literature [47], this effect disappeared when the number of cigarettes smoked on the day of testing and time since the last cigarette were taken into account. However, the present evaluation, which does take into account the number of cigarettes smoked and the time of the sample relative to the time the last cigarette was smoked, still shows an effect of age. The reasons for this apparent discrepancy are not known and warrant further evaluation.

In conclusion, the pharmacokinetics of COHb in the current analysis were best described by a two-compartment model with zero-order input and first-order elimination. The covariates that influenced COHb percent saturation were IBW for k_{12}, and FTC and age for F1. Specifically, the model suggested that F1 for COHb increased with increasing FTC and age, and that there was also a positive relationship between COHb k_{12} and IBW. The model developed may be useful in predicting COHb concentrations in adult smokers and can be used to determine optimum COHb sampling times in future studies.

Competing interests:
H-J.R. and M.S. are Philip Morris employees. D.R.M. and C.C. are consultants to Philip Morris.

All financial support was provided by Philip Morris.

References

1 Green CR, Rodgman A. The Tobacco Chemists' Research Conference: a half century forum for advances in analytical methodology of tobacco and its products. Recent Adv Tobacco Sci 1996; 22: 131–304.

2 Report by the Surgeon General. The Health Consequences of Smoking. Executive Summary: A Report of the Surgen General. Washington, DC: U.S. Public Health Services 2004.

3 Haab P. The effect of carbon monoxide on respiration. Experientia 1990; 46: 1202–6.

4 Salhany JM. Effect of carbon dioxide on human hemoglobin. Kinetic basis for the reduced oxygen affinity. J Biol Chem 1972; 247: 3799–801.

5 Roughton FJ, Darling RC. The effect of carbon monoxide on the oxyhemoglobin dissociation curve. Am J Physiol 1944; 141: 17–31.

6 Caughey WS. Carbon monoxide bonding in hemeproteins. Ann NY Acad Sci 1970; 174: 148–53.

7 Peterson JE, Stewart RD. Predicting the carboxyhemoglobin levels resulting from carbon monoxide exposures. J Appl Physiol 1975; 39: 633–8.

8 Andersen ME, Clewell HJ III, Gargas ML, MacNaughton MG, Reitz RH, Nolan RJ, McKenna MJ. Physiologically based

pharmacokinetic modeling with dichloromethane, its metabolite, carbon monoxide, and blood carboxyhemoglobin in rats and humans. Toxicol Appl Pharmacol 1991; 108: 14–27.
9 Bruce EN, Bruce MC. A multicompartment model of carboxyhemoglobin and carboxymyoglobin responses to inhalation of carbon monoxide. J Appl Physiol 2003; 95: 1235–47.
10 Jones RM, Fagan R. Carboxyhemoglobin in nonsmokers: a mathematical model. Arch Environ Health 1975; 30: 184–9.
11 Coburn RF, Forster RE, Kane PB. Considerations of the physiological variables that determine the blood carboxyhemoglobin concentration in man. J Clin Invest 1965; 44: 1899–910.
12 Peterson JE, Stewart RD. Absorption and elimination of carbon monoxide by inactive young men. Arch Environ Health 1970; 21: 165–71.
13 Roethig HJ, Kinser RD, Lau RW, Walk RA, Wang N. Short-term exposure evaluation of adult smokers switching from conventional to first-generation electrically heated cigarettes during controlled smoking. J Clin Pharmacol 2005; 45: 133–45.
14 Pillsbury HC, Bright CC. Comparison of aliquot and complete sample procedure for the determination of nicotine in cigarette smoke. J Assoc Off Anal Chem 1972; 55: 636–8.
15 Law MR, Morris JK, Watt HC, Wald NJ. The dose–response relationship between cigarette consumption, biochemical markers and risk of lung cancer. Br J Cancer 1997; 75: 1690–3.
16 Devine D. Case study number 25 gentamicin therapy. Drug Intell Clin 1974; 8: 650–5.
17 Sheiner BL, Beal SL. Evaluation of methods for estimating population pharmacokinetic parameters. II. Biexponential model and experimental pharmacokinetic data. J Pharmacokinet Biopharm 1981; 9: 635–51.
18 Sheiner LB, Beal S, Rosenberg B, Marathe VV. Forecasting individual pharmacokinetics. Clin Pharmacol Ther 1979; 26: 294–305.
19 Wahlby U, Jonsson EN, Karlsson MO. Assessment of actual significance levels for covariate effects in NONMEM. J Pharmacokinet Pharmacodyn 2001; 28: 231–52.
20 Gobburu JV, Lawrence J. Application of resampling techniques to estimate exact significance levels for covariate selection during nonlinear mixed effects model building: some inferences. Pharm Res 2002; 19: 92–8.
21 Mandema JW, Verotta D, Sheiner LB. Building population pharmacokinetic–pharmacodynamic models. I. Models for covariate effects. J Pharmacokinet Biopharm 1992; 20: 511–28.
22 Yafune A, Ishiguro M. Bootstrap approach for constructing confidence intervals for population pharmacokinetic parameters. I. A use of bootstrap standard error. Stat Med 1999; 18: 581–99.
23 Yano Y, Beal SL, Sheiner LB. Evaluating pharmacokinetic/pharmacodynamic models using the posterior predictive check. J Pharmacokinet Pharmacodyn 2001; 28: 171–92.
24 Ette EI, Onyiah LC. Estimating inestimable standard errors in population pharmacokinetic studies: the bootstrap with Winsorization. Eur J Drug Metab Pharmacokinet 2002; 27: 213–24.
25 Shete S, Beasley TM, Etzel CJ, Fernandez JR, Chen J, Allison DB, Amos CI. Effect of winsorization on power and type 1 error of variance components and related methods of QTL detection. Behav Genet 2004; 34: 153–9.
26 Roughton FJ. Kinetics of gas transport in the blood. Br Med Bull 1963; 19: 80–9.
27 Coburn RF, Williams WJ, White P, Kahn SB. The production of carbon monoxide from hemoglobin *in vivo*. J Clin Invest 1967; 46: 346–56.
28 Blomberg LM, Blomberg MR, Siegbahn PE. A theoretical study on the binding of O(2), NO and CO to heme proteins. J Inorg Biochem 2005; 99: 949–58.
29 Lim M, Jackson TA, Anfinrud PA. Binding of CO to myoglobin from a heme pocket docking site to form nearly linear Fe-C-O. Science 1995; 269: 962–6.
30 Omura T, Sato R, Cooper DY, Rosenthal O, Estabrook RW. Function of cytochrome P-450 of microsomes. Fed Proc 1965; 24: 1181–9.
31 Hill BC. The pathway of CO binding to cytochrome c oxidase. Can the gateway be closed? FEBS Lett 1994; 354: 284–8.
32 Yoshikawa S, Choc MG, O'Toole MC, Caughey WS. An infrared study of CO binding to heart cytochrome c oxidase and hemoglobin A. Implications re O2 reactions. J Biol Chem 1977; 252: 5498–508.
33 Shimazu T, Ikeuchi H, Sugimoto H, Goodwin CW, Mason AD Jr, Pruitt BA Jr. Half-life of blood carboxyhemoglobin after short-term and long-term exposure to carbon monoxide. J Trauma 2000; 49: 126–31.
34 Muranaka H, Higashi E, Itani S, Shimizu Y. Evaluation of nicotine, cotinine, thiocyanate, carboxyhemoglobin, and expired carbon monoxide as biochemical tobacco smoke uptake parameters. Int Arch Occup Environ Health 1988; 60: 37–41.
35 Turner JA, McNicol MW, Sillett RW. Distribution of carboxyhaemoglobin concentrations in smokers and non-smokers. Thorax 1986; 41: 25–7.
36 Wagner JA, Horvath SM, Dahms TE. Carbon monoxide elimination. Respir Physiol 1975; 23: 41–7.
37 Weaver LK, Howe S, Hopkins R, Chan KJ. Carboxyhemoglobin half-life in carbon monoxide-poisoned patients treated with 100% oxygen at atmospheric pressure. Chest 2000; 117: 801–8.
38 Piantadosi CA. Carbon monoxide poisoning. Undersea Hyperb Med 2004; 31: 167–77.
39 Myers RA, Snyder SK, Emhoff TA. Subacute sequelae of carbon monoxide poisoning. Ann Emerg Med 1985; 14: 1163–7.
40 Burney RE, Wu SC, Nemiroff MJ. Mass carbon monoxide poisoning: clinical effects and results of treatment in 184 victims. Ann Emerg Med 1982; 11: 394–9.
41 Pace N, Strajman E, Walker EL. Acceleration of carbon monoxide elimination in man by high pressure oxygen. Science 1950; 111: 652–4.

42 McArdle WD, Katch FI, Katch VL. Exercise Physiology: Energy Nutrition, and Human Performance. 2nd edn. Chapter 14 part 2. Philadelphia, PA: Lea & Febiger 1986.

43 Nordenberg D, Yip R, Binkin NJ. The effect of cigarette smoking on hemoglobin levels and anemia screening. JAMA 1990; 264: 1556–9.

44 Guyton AC. Basic Human Physiology: Normal Function and Mechanisms of Disease, 2nd edn. Chapter 28. Philadelphia, PA: W.B. Saunders, Co. 1977.

45 Mathews CK, van Holde KE. Biochemistry, Chapter 7. Redwood City, CA: Benjamin/Cummings Publications Co. Inc. 1990:

46 Griffen KI. Medical Information: Carbon Monoxide Poisoning; New Thinking about an Old Toxin. Tracker 2004; 7: 10–12.

47 McNeill AD, West R, Jarvis MJ, Russell MA. Do older children take in more smoke from their cigarettes? Evidence from carbon monoxide levels. J Behav Med 1986; 9: 559–65.